Cell, Vol. 91, 777–788, December 12, 1997, Copyright ©1997 by Cell Press

Drosophila Ecdysone Receptor Mutations Reveal Functional Differences among Receptor Isoforms

Michael Bender,*† Farhad B. Imam,* William S. Talbot,*§ Barry Ganetzky,‡ and David S. Hogness*||
*Departments of Developmental Biology and Biochemistry
Stanford University Medical Center
Stanford, California 94305
†Department of Genetics
University of Georgia
Athens, Georgia 30602
‡Laboratory of Genetics
University of Wisconsin-Madison
Madison, Wisconsin 53706

Summary

The steroid hormone ecdysone directs Drosophila metamorphosis via three heterodimeric receptors that differ according to which of three ecdysone receptor isoforms encoded by the *EcR* gene (EcR-A, EcR-B1, or EcR-B2) is activated by the orphan nuclear receptor USP. We have identified and molecularly mapped two classes of *EcR* mutations: those specific to EcR-B1 that uncouple metamorphosis, and embryonic-lethal mutations that map to common sequences encoding the DNA- and ligand-binding domains. In the larval salivary gland, loss of EcR-B1 results in loss of activation of ecdysone-induced genes. Comparable transgenic expression of EcR-B1, EcR-B2, and EcR-A in these mutant glands results, respectively, in full, partial, and no repair of that loss.

Introduction

Among the thirteen Drosophila melanogaster genes that encode nuclear receptors containing both DNA-binding (DBD) and ligand-binding (LBD) domains (Thummel, 1995), the ecdysone receptor gene, *EcR*, is the only one known to encode a ligand-activated receptor (Koelle et al., 1991). Indeed, *EcR* encodes three such receptors, the EcR-A, EcR-B1, and EcR-B2 isoforms that contain the same DBD and LBD, differing only in their N-terminal regions (Talbot et al., 1993, Figure 1B). The remaining twelve genes encode orphan receptors for which activating ligands have not yet been identified or do not exist. One of these orphan receptors, USP, exhibits a strong structural and functional similarity to the vertebrate RXR receptors. Like the RXR receptors, which form heterodimers with the nonsteroid receptors for thyroid hormone, retinoic acid, and vitamin D, and thereby activate them for DNA binding (Mangelsdorf and Evans, 1995), the USP receptor interacts with each of the EcR isoforms to form DNA-binding heterodimers (Koelle, 1992; Yao et al., 1992; M. N. Arbeitman, M. R. Koelle and D. S. H., unpublished data). The Drosophila EcR receptors are thus akin to the rapidly expanding vertebrate family of RXR heteromeric receptors (Mangelsdorf and Evans, 1995), rather than to the smaller vertebrate family of steroid hormone receptors that bind DNA as homodimers (Beato et al., 1995). This is curious because the EcR ligand is the steroid hormone 20-hydroxyecdysone, referred to here as ecdysone. Indeed, some have taken this situation to indicate that the vertebrate steroid receptor family, once considered the archetype of the nuclear receptors, is instead a recently evolved branch of that superfamily (Mangelsdorf et al., 1995).

The Drosophila ecdysone receptors and the genetic networks that they activate provide an attractive model system for the analysis of how the RXR family of receptors can control complex developmental processes. One attraction is the genetic simplicity of the EcR-USP system relative to that of the vertebrate RXR systems. For example, the *ultraspiracle* (*usp*) gene encodes only one protein, USP, which is the only known Drosophila homolog of the vertebrate RXRs. By contrast, in mammals four RXR isoforms are encoded from three genes (Giguere, 1994). Similarly, in Drosophila there is but one ecydysone receptor gene that encodes three isoforms, whereas in mammals there are three retinoic acid receptor genes (RARα, -β, and -γ) that encode eight isoforms and two thyroid hormone receptor genes (TRα and -β) that encode four isoforms (Refetoff et al., 1994; Kastner et al., 1995). Thus, the possible number of different RAR/RXR and TR/RXR heterodimers are, respectively, eleven and five times the three EcR/USP heterodimers.

Another simplifying feature of the EcR/USP system is that the principal temporal determinant for its activation throughout the animal is a series of ecdysone pulses, which, with the exception of a midembryonic pulse, derive from the prothoracic gland in response to a neuropeptide signal from the brain (Riddiford, 1993). The first two of these prothoracic pulses induce the molts that punctuate the ends of the first two of the three larval instars. Metamorphosis to the adult fly is then triggered by a late-larval pulse that peaks at the larval-to-prepupal transition (pupariation). It is further controlled by a small prepupal pulse that peaks 10 hr later, just before the prepupal-to-pupal transition (pupation), and by a large pupal pulse—most studies having focused on the metamorphic stages controlled by the late-larval and prepupal pulses.

These pulses induce widely different metamorphic responses in the different ecdysone target tissues, which include virtually all larval and imaginal tissues. Thus, the imaginal discs evert to the outside surface to form rudimentary adult appendages, their edges then extending and joining to form a continuous epithelium for the adult head and thorax. These pulses also induce the proliferation of small clusters of imaginal cells (histoblasts), which will form the abdominal epithelium of the adult (Fristrom and Fristrom, 1993). Similar but less well-studied differences exist in the ecdysone response of imaginal tissues that form the adult gut and salivary glands. Thus, the adult midgut is formed from imaginal

§Present address: Developmental Genetics Program, Skirball Institute, NYU Medical Center, New York, New York 10016.
||To whom correspondence should be addressed.

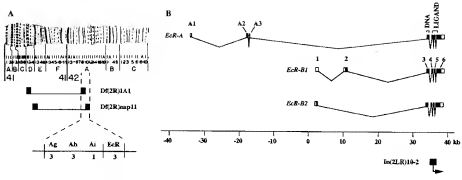

Figure 1. Genetic and Physical Maps of the *EcR* Locus

(A) The extents of *Df(2R)1A1* and *Df(2R)nap11* are indicated by horizontal lines shown relative to the second chromosome polytene banding pattern of regions 41 and 42. Shaded boxes indicate the resolution of the deletion endpoints. The *EcR* gene lies within the interval indicated by dashed lines. Complementation groups (Ag, Ah, Ai, and EcR) within this interval and the number of alleles in each group are indicated at bottom. The *EcR* group has been localized to the right end of this interval by deletion mapping. (B) The structures of the three *EcR* mRNAs (figure modified from Talbot et al., 1993) are shown above the line. Protein coding sequences are indicated by black boxes. DNA- and ligand-binding domains are designated. The position of the inversion breakpoint of the $EcR^{In(2LR)10-2}$ mutation is indicated below the line.

histoblasts that are induced by the late-larval pulse to propagate and spread out to form the adult structure, whereas the adult foregut, hindgut, and salivary glands derive from single large clusters of cells called imaginal rings (Skaer, 1993). By contrast, most larval cells undergo apoptosis induced by the late-larval pulse in some tissues and by the prepupal pulse in others (Jiang et al., 1997).

The expression patterns of the EcR-A and EcR-B1 isoforms among the ecdysone target tissues at puparíation provide another simplifying characteristic of the EcR/USP system (Talbot et al., 1993; the EcR-B2 pattern has not yet been determined for lack of an antibody against the 17 aa B2-specific region). The EcR-A isoform predominates in the imaginal discs, imaginal rings, and in two sets of specialized larval cells that postpone their deaths to provide late metamorphic functions: namely, the prothoracic gland cells (Dai and Gilbert, 1991; Talbot et al., 1993) and the type II larval neurons of the central nervous system (Robinow et al., 1993). The EcR-B1 isoform, by contrast, predominates in the other larval tissues and in the imaginal histoblasts that form the abdominal epithelium and the midgut of the adult (Talbot et al., 1993). Hence, tissues belonging to a given metamorphic class, such as the imaginal discs, exhibit the same isoform expression pattern, which is usually characterized by a strong predominance of one isoform.

This predominance induces the expectation that mutants lacking the A or B1 isoform at puparíation will exhibit metamorphic defects specific to tissues in which the respective isoforms predominate. In this paper, we show that this is indeed the case for *EcR-B1* mutants in which the B1 isoforms are truncated by stop codons near their amino termini. This result contrasts with that obtained by RAR knockouts in mice, where the knockout of a pair of isoforms is required to obtain the expected defects—single-isoform knockouts producing little or no defects (Kastner et al., 1995). The rationale for this result is that one RAR isoform can substitute for another as long as a sufficient isoform abundance exists. Our *EcR-B1* mutant results do not address the question of whether such a functional redundancy may exist among the EcR isoforms because the residual EcR-A and/or EcR-B2 abundance in the affected tissues of the *EcR-B1* mutants could be insufficient.

We have addressed the problem of functional specificity of the EcR isoforms by testing the ability of each isoform to activate a set of genes in the larval salivary glands of an *EcR-B1* mutant when expressed from transgenes under heat-shock control. These genes exhibit a primary response to the late-larval ecdysone pulse in wild-type glands but are not activated in the *EcR-B1* mutant. Using this system, we show that the B1 isoform fully activates these primary response genes. By contrast, the A isoform fails to activate these genes, and the B2 isoform only partially activates some of them. Finally, we report the isolation and analysis of 29 other *EcR* lethal mutations and one leaky mutation in addition to the two EcR-B1 specific mutations.

Results

Identification of *EcR* Mutants

EcR has been mapped to position 42A in the polytene chromosomes by in situ hybridization (Koelle et al., 1991). A genetic map of this region is shown in Figure 1A. Hybridization of *EcR* genomic clones to Southern blots of genomic DNA from flies heterozygous for deficiencies in this region showed that *EcR* is deleted by *Df(2R)nap11* but not by *Df(2R)1A1* and that, therefore, the *EcR* gene lies within the 42A7-12 interval defined by the right endpoints of these two deficiencies (Figure 1A). Four lethal complementation groups have been defined within this region. Hybridization of cloned *EcR* DNA to Southern blots of genomic DNA from mutants within the region showed that an inversion breakpoint of one of these mutants, *In(2LR)10-2*, lies in the *EcR* gene (Figure 1B). This demonstrates that the right-most complementation group in the 42A7-12 interval corresponds to *EcR*. This group consists of $EcR^{In(2LR)10-2}$ and two other

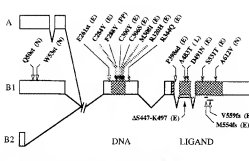

Figure 2. Molecular Map of *EcR* Mutations

Sequence changes were determined for 17 mutants that completely fail to complement and 1 leaky mutant (EcR^{W483T}) that partially fails to complement an *EcR* null mutant. Only protein coding sequences are drawn. The different amino terminal domains are nonoverlapping (see Figure 1B) and are encoded by exons A2 and A3 (EcR-A protein), exon 2 (EcR-B1 protein), and exon 1 (EcR-B2 protein) while the common carboxy terminal domain is encoded by exons 3–6. Closed arrows indicate missense mutations and one deletion that retains the normal open reading frame; open arrows indicate mutations that lead to truncation or frameshift of the *EcR* open reading frames. The extent of three small deletions is indicated by bars beneath the schematic. DNA-binding and ligand-binding domains are highlighted by striped boxes. Amino acid numbering is with respect to the EcR-B1 open reading frame (Koelle et al., 1991). The first affected amino acid residue of a mutant allele is followed by the mutant change (st = stop, fs = frame shift, sd = splice donor). The mutant class of each *EcR* mutation (Table 2) follows the mutant designation in parentheses. E = early, N = nonpupariating, PP = prepupal, L = leaky.

alleles, EcR^{C300Y} and EcR^{M554fs} (Figure 2). The $EcR^{W(CLR)10-2}$ inversion breakpoint interrupts all three *EcR* isoforms, suggesting that it inactivates all *EcR* functions. The three *EcR* mutations exhibit the same phenotype (Figure 3B) when heterozygous to an *EcR* deficiency; furthermore, the phenotype of any pairwise heterozygous combination of these alleles, as well as that of EcR^{M554fs} homozygotes, is equivalent to this phenotype. The three original *EcR* alleles are therefore null mutants.

To obtain additional mutants, we screened for ethylmethanesulfonate (EMS)–induced *EcR* mutants by noncomplementation of EcR^{C300Y}, EcR^{M554fs}, $EcR^{W(CLR)10-2}$, or a deficiency lacking *EcR* function (*Df(2R)20B*). From 21,177 mutagenized second chromosomes, we recovered 27 mutants that completely fail to complement *EcR* mutants for viability. These mutants, along with the three *EcR* alleles discussed above and EcR^{W483T}, provided by D. Segal, bring the number of alleles in this class to 31. A second class of mutants identified in this screen partially fails to complement *EcR* nulls for viability or is viable but results in a visible phenotype. One of these leaky mutants, EcR^{W483T}, was identified as an *EcR* mutant by molecular mapping (Figure 2 and Table 1).

Most of the Mapped Mutations Alter Codons for the DBD and LBD, but Two Are Specific for EcR-B1

We mapped the *EcR* mutations that alter coding sequences by denaturing gradient gel electrophoresis (DGGE) (Myers et al., 1987) followed by sequencing. Changes in gradient gel-banding patterns were seen for 21 of the 30 lethal *EcR* mutants tested. Of the 21, 17 were mapped by DNA sequencing to the positions shown in Figure 2, as was the leaky mutant EcR^{W483T}. Table 1 shows the changes in sequence for these 18 mutations.

Two mutations (EcR^{Q50st} and EcR^{W53st}) are specific to the EcR-B1 isoform (Figure 2). Both generate stop codons that lie within the EcR-B1-specific exon 2 (Figure 1B) and are predicted to produce EcR-B1 proteins truncated after only 49 (EcR^{Q50st}) or 52 (EcR^{W53st}) amino acid residues. Because neither mutation interferes with the synthesis or structure of EcR-A or EcR-B2, they should provide a means for determining EcR-B1-specific functions.

The remaining *EcR* mutations shown in Figure 2 lie within common exons (exons 3–6, Figure 1B) and therefore affect all three isoforms. These mutations divide into two groups. One consists of the four mutations that

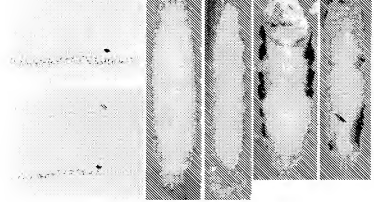

Figure 3. Terminal Phenotypes of *EcR* Mutants

Phenotypes of *EcR* early (B), nonpupariating (D), and prepupal (F) mutants are shown in comparison to wild-type animals at similar developmental stages (A, C, and E). (A and B) High magnification view of the third thoracic (open arrows) and first abdominal (closed arrows) denticle belts of the wild-type (*Canton-S*) (A) and an *EcR* early mutant (EcR^{M554fs}/*Df(2R)nap11*) (B). (C and D) A wild-type late third instar larva (*Canton-S*) (C) is compared to a late-stage *EcR* nonpupariating mutant (EcR^{C300Y}/EcR^{M554fs}) (D). White arrows indicate regions of contraction from the larval cuticle. (E and F) A wild-type animal (*Canton-S*) 12 hr after pupariation is shown in (E). Head (h), thorax (th), and abdomen (ab) can be distinguished within the pupal case. (F) shows a prepupal *EcR* mutant (EcR^{W483T}/EcR^{M554fs}). The white arrow indicates failure of anterior spiracle eversion. The black arrow indicates partial separation of the prepupa from the pupal case.

Table 1. *EcR* Mutations

Mutant	Mutation
Q50st	CAG to TAG
W53st	TGG to TAG
E261st	GAG to TAG
C284Y	TGC to TAC
F288Y	TTT to TAT
C300Y	TGC to TAC
C306S	TGC to AGC
M308I	ATG to ATA
R320H	CGC to CAC
R344Q	CGG to CAG
P398sd	G/gt to G/ga
ΔS447-K497	167 nt deletion
A483T	GCG to ACG
D491N	GAC to AAC
S531T	TCT to ACT
M554fs	22 nt deletion
V559fs	37 nt deletion
A612V	GCA to GTA
In(2LR)10-2	inversion

truncate the isoforms (open arrows, Figure 2): EcR^{E261st} generates a stop codon just upstream of the DBD, EcR^{P398sd} truncates within the LBD by altering the conserved splice donor site dinucleotide downstream of exon 4, and EcR^{M554fs} and EcR^{V559fs} are short deletions (Table 1) that result in frameshifts within the LBD. The second group consists of 11 missense mutations and a deletion that maintains the reading frame (closed arrows). Of the mutations in this group, 11 or 92% map to the DBD or LBD. The exception, EcR^{R344Q}, maps just downstream of the DBD within a conserved arginine/lysine-rich motif. Consistent with the concentration of missense mutations in the DBD and LBD, one or both of these domains are also altered by the four mutations in the first group. Although not sequenced, the remaining 4 mutations in the group of 21 exhibited altered DGGE patterns that placed them in the common region. More precisely, two ($EcR^{B1.2}$ and EcR^{B82}) could be placed in exon 3, which contains the DBD, one (EcR^{W53}) in exon 5, which consists of LBD codons, and the last (EcR^{K1}) in exon 6, which consists of LBD and 3′ terminal codons (Figures 1B and 2).

EcR Null Mutants Die during Embryogenesis While *EcR-B1* Mutants Die during Metamorphosis

Table 2 shows the percent of mutants surviving to a given stage when heterozygous to EcR^{M554fs}, a null mutation. The 29 mutants tested were scored for viability at hatching, at first, second, and third larval stages, at pupariation, and as adults, and thereby placed in three classes, which we term early, nonpupariating, and prepupal (Table 2).

Most *EcR* mutations that map to the common region (80%) are embryonic lethals of the early class (Table 2). Mutants inferred to be nulls because they eliminate or alter large segments of the DBD and/or LBD (EcR^{E261st}, EcR^{P398sd}, $EcR^{\Delta S447\text{-}K497}$, EcR^{M554fs}, EcR^{V559fs}, and $EcR^{In(2LR)10\text{-}2}$) exhibit this phenotype as do the putative nulls resulting from missense mutations in the codons for the conserved cysteines of the DBD (EcR^{C284Y}, EcR^{C300Y}, and EcR^{C306S}) (Figure 2). While some missense mutations affecting other highly conserved amino acids of the DBD (EcR^{R320H}) or LBD (EcR^{D491N}) are also in the early class, this is not always the case, as exemplified by EcR^{F288Y}, which alters a highly conserved phenylalanine in the DBD yet is in the prepupal class (Table 2). Reciprocally, a few mutations affecting residues that are not highly conserved (EcR^{M308I}, EcR^{R344Q}, and EcR^{S531T}) fall into the early class, as do three of the mutations mapped only to exon resolution ($EcR^{B1.2}$, EcR^{K1}, and EcR^{B82}), the fourth (EcR^{APP2}) not having been tested. The remaining five early mutations (EcR^{K1}, EcR^{MM1}, EcR^{R1H2}, EcR^{KF1}, and EcR^{KX4}) were not localized by DGGE and may lie outside of the coding region.

The *EcR* early null mutants $EcR^{In(2LR)10\text{-}2}$, EcR^{C300Y}, and EcR^{M554fs} form a largely normal cuticle, which bears the proper number of ventral denticle belts. A number of more subtle defects are, however, characteristic of these mutants, including reductions in denticle size and number (Figure 3B, arrows) and occasional mouthpart aberrancies. It should be noted that a maternal contribution of *EcR-A* mRNA and protein has been observed (Talbot et al., 1993; J. Hiebert and D. S. H., unpublished data); hence, the phenotype of a full null *EcR* is apt to be more severe.

The *EcR* nonpupariating and prepupal mutant classes affect the early stages of metamorphosis, which commences with pupariation, the formation of the pupal case. Pupariation is preceded by a cessation of wandering and includes shortening of the larva, eversion of anterior spiracles, attachment to a solid surface, and hardening of the cuticle (compare Figures 3C and 3E). Separation of the larval cuticle from the underlying epidermis (the larval/pupal apolysis) takes place 4 to 6 hr after puparium formation (APF) and is followed by the prepupal ecdysone pulse at 10 hr APF. Head eversion, the landmark used to divide the prepupal and pupal stages, follows at 12 hr APF.

Both *EcR-B1* mutants (EcR^{Q50st} and EcR^{W53st}) are members of the nonpupariating class (Table 2). They initiate wandering but fail to evert spiracles, shorten, attach themselves to a solid surface, or harden their cuticle. Despite failure of these earlier events, the *EcR-B1* mutants easily slip free of the larval cuticle when dissected, indicating that apolysis of the larval cuticle has been completed, and hence, that coordination of the early events of metamorphosis is disrupted. The terminal phenotype of the *EcR-B1* mutant EcR^{Q50st}/EcR^{M554fs} is shown in Figure 3D. Three other members of the nonpupariating class (EcR^{RC1}, EcR^{R10}, and EcR^{rig21}) show a similar lethal phase (Table 2) and similar terminal phenotypes, suggesting that these three mutants may also lack *EcR-B1* function.

Three *EcR* common exon mutants (EcR^{F288Y}, EcR^{M483T}, and EcR^{A612V}) are not members of the early class and may, therefore, be weak loss-of-function mutants. One of these (EcR^{A612V}) falls into the nonpupariating class, although its terminal phenotype is distinct from the *EcR-B1* mutants and other members of this class. EcR^{A612V} mutants do not wander and generally die as early third instar larvae. The second of these exceptional mutants (EcR^{M483T}) is leaky as it partially complements an *EcR* null mutant. The third (EcR^{F288Y}) is a member of the prepupal class, which is characterized by substantial levels of pupariation but little or no adult survival (Table 2). The terminal phenotype of EcR^{F288Y}/EcR^{M554fs} is shown in Figure 3F. Mutants of this class form a hardened puparium

Table 2. *EcR* Lethal Phase

Paternal Allele	Percent Survival					
	Hatched	1st Larval	2nd Larval	3rd Larval	Pupal	Adult
cn bw (Parental)	78	78	74	72	72	64
Early						
E261st	2	0	—	—	—	—
C284Y	6	0	—	—	—	—
C306S	2	0	—	—	—	—
M308I	4	0	—	—	—	—
R344Q	6	0	—	—	—	—
P398sd	2	0	—	—	—	—
ΔS447-K497	4	0	—	—	—	—
D491N	2	0	—	—	—	—
M554fs	0	0	—	—	—	—
V559fs	0	0	—	—	—	—
In(2LR)10-2	0	0	—	—	—	—
3L2	0	0	—	—	—	—
6K1	0	0	—	—	—	—
5MM1	0	0	—	—	—	—
6HH2	2	0	—	—	—	—
4FF1	18	0	—	—	—	—
R320H	36	2	0	—	—	—
4X4	52	8	0	—	—	—
5K1	54	10	0	—	—	—
6B2	50	26	0	—	—	—
S531T	52	8	2	0	—	—
Nonpupariating						
A612V	42	36	34	16	0	—
Q50st	64	64	62	36	0	—
W53st	82	82	70	54	0	—
3C1	74	74	68	62	0	—
6II3	84	84	74	74	0	—
lig21	98	98	94	94	0	—
Prepupal						
F288Y	56	56	48	38	36	0
4DD1	74	74	70	62	36	2

EcR mutants heterozygous to the null allele EcR^{M554fs}, recognizable by the *y* marker, were scored for survival at six times during development. Percent survival is expressed as a percentage of the *y* animals expected (50 animals) from a collection of 200 eggs (see Experimental Procedures) at the following stages: hatching; first, second, and third larval; pupal, and adult. Mutants in the early, nonpupariating, and prepupal classes are separated by spaces. The early class is subdivided into strong (probable null) and weak (hypomorphic) alleles by a space. Mutants in bold type have been defined at the molecular level, including EcR^{W53st}, EcR^{E10-2}, EcR^{3L2}, EcR^{6K1}, and EcR^{6B2}, which, though not mapped to the nucleotide, have been mapped to the common region.

that is generally misshapen and spiracle eversion is often abnormal (Figure 3F, white arrow). Most *EcR* prepupal mutants separate from the pupal case (Figure 3F, black arrow), indicating that the larval/pupal apolysis has begun. Head eversion, however, generally does not occur, indicating a late prepupal lethal period.

EcR-B1 Mutants Exhibit Defects in Specific Tissue Classes

To test the simple prediction that metamorphosis in *EcR-B1* mutants will be defective in tissues where EcR-B1 predominates, we examined four tissues of this sort in an *EcR-B1* mutant (EcR^{W53st}/EcR^{M554fs}), comparing them to a control tissue in which EcR-A predominates. The four EcR-B1-predominant tissues were the larval midgut, the midgut imaginal islands, the abdominal histoblasts that give rise to the adult abdomen, and the larval salivary glands, whereas the leg imaginal discs served as the EcR-A-predominant control tissues (Talbot et al., 1993).

Approximately 6 hr prior to puparium formation, the imaginal discs begin a process of elongation and eversion that is induced by the late-larval ecdysone pulse. This process can most easily be followed in the leg imaginal discs. By 3 hr APF, the individual tarsal segments of the leg are visible, and by 6 hr APF, spreading and fusion of the discs has begun, a process that is completed 4–5 hr later (Fristrom and Fristrom, 1993). Figure 4A shows a wild-type leg disc taken from a prepupa 6 hr APF. In late-stage *EcR-B1* mutants, leg discs show clear evidence of elongation (Figure 4B), and in some animals fusion of these discs takes place. Thus, this EcR-A-predominant control initiates its normal metamorphic response in *EcR-B1* mutants. Disc elongation in *EcR-B1* mutants also confirms the suggestion given in the preceding section that apolysis of the larval cuticle is completed in these mutants since disc elongation requires this apolysis (Fristrom and Fristrom, 1993).

EcR-B1 is the predominant isoform in both the imaginal and larval cells of the larval midgut; indeed, the imaginal cells do not express detectable EcR-A (Talbot et al., 1993). Figure 5A shows the large polyploid cells

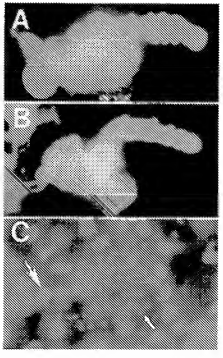

Figure 4. Phenotype of an *EcR-B1* Mutant Imaginal Disc and Histoblast Nest

DAPI-stained tissues from the wild-type (*Canton-S*) (A) and an *EcR-B1* mutant (EcR^{W3ns}/EcR^{M554fs}) (B) are shown. (A) Leg disc from a wild-type prepupa 6 hr after pupariation. Elongation of the disc to form the leg has taken place and individual tarsal segments of the leg can be distinguished. (B) Leg disc from a late-stage *EcR-B1* mutant. (C) Ventral histoblast nest (small nuclei, small arrow) consisting of 62 cells from a late-stage *EcR-B1* mutant. Large nuclei (large arrow) are polytene larval nuclei. (see Experimental Procedures for staging of *EcR-B1* mutant animals).

(large arrow) of the larval epithelial layer that lines the lumen of the midgut. Interspersed with these larval cells are the midgut imaginal islands (small arrows), small groups of diploid cells that will give rise to the adult gut. Within 2 hr APF, the cells of the midgut imaginal islands begin to proliferate. Ultimately the islands join to form a complete tube (Figure 5B, small arrow). During this process, the larval cells coalesce into a compact mass (Figure 5B, large arrow) in the lumen of the adult gut. Neither cell type follows its normal developmental pathway at metamorphosis in *EcR-B1* mutants. The imaginal cells of the midgut islands begin to proliferate (Figure 5C, small arrow) but fail to form a tube surrounding the larval epithelial cells, and the larval epithelial cells fail to become condensed into a compact mass (Figure 5C, large arrow). Cell–cell contacts between these two cell types cloud the issue somewhat because it is difficult to judge whether failure of ecdysone response in one cell type might influence the other cell type. Nevertheless, it appears that normal ecdysone responses in both cell types are ultimately blocked.

The abdominal histoblasts, which give rise to the adult abdomen, express EcR-B1 but no detectable EcR-A (Talbot et al., 1993). These cells are present in the epidermis of the first through seventh abdominal segments in small nests. At pupariation, each hemisegment contains an anterior dorsal nest (15–16 cells), a posterior dorsal nest (6–7 cells), and a ventral nest (11–12 cells) (Madhavan and Madhavan, 1980). The abdominal histoblasts, like the midgut imaginal cells, undergo a strong proliferative response during metamorphosis. The histoblasts begin dividing several hours after pupariation and increase to as many as 250 cells per nest in the next 12 hr (Fristrom and Fristrom, 1993). Shortly thereafter, the histoblast nests begin to spread and replace adjacent abdominal larval cells, a replacement that is complete by 40 hr after pupariation. Counts of histoblast numbers in *EcR-B1* mutants reveal that histoblast proliferation is initiated in these animals, but no replacement of larval cells was observed. Ninety-one nests were counted from a total of six different late-stage *EcR-B1* mutants. The average number of histoblasts in the anterior dorsal nests was 58 ± 13.6 SD (n = 32 nests), in the posterior dorsal nests was 17 ± 4.4 SD (n = 28 nests), and in the ventral nests was 51 ± 8.1 SD (n = 31 nests). A representative anterior dorsal nest from an *EcR-B1* mutant is shown in Figure 4C. Thus, while histoblast proliferation is initiated in *EcR-B1* mutants, proliferation is limited to one or two cell doublings.

We tested whether the transcriptional response to ecdysone in an EcR-B1 predominant tissue was defective in an *EcR-B1* mutant by examining the response to the late-larval ecdysone pulse of four early and two early-late genes in mutant larval salivary glands. In wild-type glands, both early and early-late genes exhibit a primary response to ecdysone and when active engender puffs in the polytene chromosomes of these glands (reviewed by Russell and Ashburner, 1996). Figure 6A shows that the *BR-C*, *E74*, and *E75* early genes, represented by the puffs at 2B, 74EF, and 75B, respectively (Burtis et al., 1990; Segraves and Hogness, 1990; Dibello et al., 1991), were submaximally or negligibly induced in the *EcR-B1* mutant (EcR^{W53st}/EcR^{M554fs}) relative to the puffs produced in the *Canton-S* wild type. The relatively high value for the 2B puff in the *EcR-B1* mutant results from the fact that the *BR-C* gene exhibits significant activity before the late-larval pulse (Andres et al., 1993) and that this activity is not affected by the *EcR-B1* mutation (data not shown). Induction of the *E78* early-late gene, as represented by the 78C puff, is also much reduced in the *EcR-B1* mutants, as is the early-late puff at 62E (Figure 6A). The latter result suffers from the fact that the gene responsible for the 62E puff has not been identified, so that the relationship between transcription and puffing at this locus has yet to be defined. The significance of our finding that the early puff at 23E is equivalently induced in wild type (puff ratio = 1.6 ± 0.05 SE) and in the *EcR-B1* mutant (puff ratio = 1.5 ± 0.07 SE) is similarly open to question because the gene responsible for this puff has been cloned, but the exact relationship between its transcription and puffing is yet to be determined (D. Garza and D. S. H., unpublished data).

EcR Rescue of Defective Puffing in an *EcR-B1* Mutant Is Isoform-Specific

Evidence that the EcR isoforms are functionally distinct derived from experiments in which we tested each isoform for its ability to activate early and early-late genes

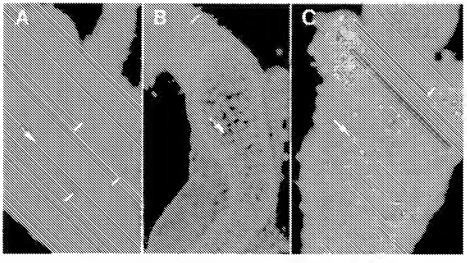

Figure 5. Phenotypes of *EcR-B1* Mutant Midgut Tissues

DAPI-stained tissues from the wild-type (Canton-S; A and B) and an *EcR-B1* mutant (EcR^{M534}/EcR^{M554fs}; C) are shown. (A and B) The anterior midgut from a wild-type late third instar larva (A) and from a wild-type animal 12 hr after pupariation (B). (C) The anterior midgut from a late-stage *EcR-B1* mutant (see Experimental Procedures for staging of *EcR-B1* mutant animals). In (A), (B), and (C), the large nuclei of the polyploid larval cells are indicated by large arrows, and the small nuclei of the diploid midgut imaginal islands are indicated by small arrows.

made dormant in larval salivary glands by *EcR-B1* mutations. To that end, we generated transgenic lines carrying a heat-shock promoter fused to the open reading frame of each EcR isoform and crossed them into *EcR-B1* mutant backgrounds. The three early genes at 2B (*BR-C*), 74EF (*E74*), and 75B (*E75*), and the two early-late genes at 62E and 78C (*E78*) were tested for their response to the late-larval ecdysone pulse after the heat-shock induction of each EcR isoform in test strains of the following genotype: *yw*; EcR^{M532s}/EcR^{M554fs}; *hs EcR-x*/+, where *x* is A, B1, or B2. We also tested the early genes responsible for the early puff at 63F (*E63–1* and *E63–2*, Andres and Thummel, 1995) in the same manner. These genes and their puff are induced in a primary response to the late larval ecdysone pulse in wild-type but are not induced in the *EcR-B1* mutant EcR^{M534}/EcR^{M554fs} (Figure 6B; dark blue bar).

Figure 6B shows that the size of the puffs induced by the late-larval ecdysone pulse in the *EcR-B1* mutant after heat-shock induction of the EcR-B1 isoform (red bars) is greater than that resulting from the induction of the EcR-A (green bars) or EcR-B2 (yellow bars) isoforms, with the possible exception of the *BR-C* puff at 2B, where the difference in the EcR-B1 and EcR-B2 rescue is not significant. Indeed, the size of the puffs resulting from the expression of EcR-B1, two of which are shown in Figure 6C, are essentially the same as the puffs observed in wild-type glands (Figure 6A, blue bars), with the exception of the early-late 78C (*E78*) puff.

The heat-shock expression of EcR-B2 allows significant induction of all of the early and early-late genes examined except that of the early-late *E78* gene at 78C and possibly that of the early *BR-C* gene at 2B. In the latter case, comparison of the 2B puff sizes for the EcR^{M535s}/EcR^{M554fs} mutant control in Figures 6A and 6B suggests that heat shock may affect the appreciable levels of *BR-C* activity observed in the *EcR-B1* mutant prior to the late-larval ecdysone pulse. By contrast, the heat-shock expression of the EcR-A isoform does not allow significant ecdysone induction of any of the early or early-late puffs, with the possible exception of 63F.

The conclusion from the above data that the three EcR isoforms are functionally distinct is dependent upon the generation by heat shock of comparable nuclear abundances for the three EcR isoforms that approximate or exceed the wild-type values. We show here that this condition was met by measuring the relative nuclear abundances of the isoforms in each of the three heat-shock isoform parental lines (*yw*; $EcR^{M554fs}/CyO,y^{+}$; *hs EcR-x*/*hs EcR-x*, where *x* is A, B1, or B2), which were heat shocked at 37°C, or not, for 45 min, followed by a 3 hr recovery at 22°C. Nuclear abundance was measured by exposure of the glands to the monclonal antibody DDA2.7 against an epitope in the EcR common region, followed by staining with a fluorescein-conjugated secondary antibody and quantitative measure of the nuclear fluorescence in a confocal microsope, with results shown in Figure 6D.

The difference between the heat-shocked and non-heat-shocked values should represent the amount of the specific isoform produced from the *hs* transgene: namely, 68.9, 94.3, and 48.4 for the A, B1, and B2 isoforms, respectively. Given that the strains used to obtain the results in Figure 6B carried only one *hs EcR-x* chromosome, they should produce half the above values, or 34.4, 47.2, and 24.2. These values are to be compared to those in the non-heat-shocked column of Figure 6D, which represent the sum of the wild-type and the M554fs forms of EcR-B1, given that the epitope for the DDA2.7 antibody is between the residues 335 and 393 of EcR-B1 and that the M554fs isoform is truncated C-terminal to residue 554. The mean of these values is 18.8, which approximates the diploid or haploid wild-type concentration depending upon whether M554fs protein turns

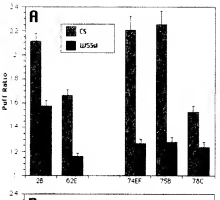

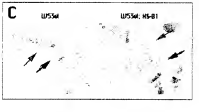

D

Strain	Heat Shock	
	–	+
HS-A	24.6 ± 8.9	95.5 ± 17.0
HS-B1	12.9 ± 1.4	187.2 ± 28.5
HS-B2	18.9 ± 8.3	67.5 ± 5.1

Figure 6. Defects in Induction of Early and Early-Late Puffs in *EcR-B1* Mutant Larvae and Rescue of these Defects by Heat-Shock Expression of EcR Isoforms

(A and B) Puff sizes in salivary glands from *EcR-B1* mutant larvae (A). The graph compares puff sizes in wild-type clear-gut larvae (*Canton-S*, abbreviated to CS, blue columns) to puff sizes in *EcR-B1* mutant clear-gut larvae (EcR^{W53st}/EcR^{M554fs}, abbreviated to W53st, green columns). In (A) and (B), each column represents the mean and standard error of twenty total puff measurements (four nuclei from each of five larvae). The puffs listed on the abscissa include both early (2BS–6, 74EF, and 75B) and early-late (62E and 78C) puffs. (B) Rescue of puffing in *EcR-B1* mutant larvae following heat-shock induction of EcR isoforms. *EcR-B1* mutant larvae (*yw*; EcR^{W53st}/EcR^{M554fs}) were used as controls (purple columns). The other three genotypes were identical to the control except for the presence of a heat-inducible EcR isoform-specific transgene (*hs EcR-A*, green columns; *hs EcR-B2*, yellow columns; and *hs EcR-B1*, red columns). The puffs listed on the abscissa include early (2B, 63F, 74EF, and 75B) and early-late (62E and 78C) puffs.

(C) Salivary gland squashes are shown for a control *EcR-B1* mutant larva (left panel) and an *EcR-B1* mutant larva carrying a copy of the *hs EcR-B1* transgene (right panel). Expression of EcR-B1 following heat-shock rescues puffing of the 74EF (black arrow) and 75B (red arrow) early genes.

(D) Relative abundance of EcR protein in larval salivary gland nuclei following heat-shock induction of *EcR* transgenes. EcR protein levels were quantitated as described in Experimental Procedures for three strains (*yw*; *EcR*W554fs/*CyO,y*$^{+}$; *hs EcR-x*/*hs EcR-x*, where *x* is A, B1, or B2) with and without heat shock. The values represent the mean and standard deviation for four nuclei for each condition.

over at the same rate as wild-type or much faster, and assuming negligible contributions of other isoforms.

Discussion

Mutational Definition of the *EcR* Gene

The two overlapping *EcR* transcription units produce three EcR isoforms because the *EcR-B* unit produces two mRNAs by alternative splicing (Figure 1). If each of the three EcR isoforms is required for viability, one would then expect a lethal complementation pattern of five groups: three groups (A, B1, and B2) that complement one another and individually inactivate one of the isoforms, one group (B) that inactivates both B isoforms and therefore complements members of the A but not B1 and B2 groups, and one group (C) that fails to complement members of any of the other groups as a result of mutation in the common region. Our data define two of these groups (B1 and C) and demonstrate the existence of at least one more (A and/or B2). The C group is defined by the first 12 mutations in Table 2 plus EcR^{E300Y}, all of which are embryonic lethals, map to the common region (Figure 2), and fail to complement one another and the two mutations that define the B1 group (EcR^{E300c} and EcR^{W53st}). Because B1/C heterozygotes (e.g., EcR^{W53st}/EcR^{M554fs}) complete embryonic development (Table 2), the EcR-A and/or EcR-B2 isoforms encoded by the B1 mutant chromosome evidently supply the embryonic functions that cannot be supplied by the C mutant chromosome. The recent isolation of a B mutant that eliminates both EcR-B1 and EcR-B2 isoforms by a small deletion covering the *EcR-B* promoter and adjacent sequences provides evidence that EcR-B2 does not supply the embryonic function, as this B mutant completes embryogenesis (M. Schubiger, A. A. Wade, G. E. Carney, J. Truman, and M. B., unpublished data). If a single EcR isoform is involved, it would, therefore, appear that the EcR-A isoform provides this embryonic function, a conclusion in keeping with its strong embryonic expression (Talbot et al., 1993). This conclusion should soon be testable via small deletion mutations in the *EcR-A* promoter region that are currently under examination (G. E. Carney and M. B., unpublished data). Given this isolation of A mutants, B2 would be the only undefined group. B2 mutants promise to be difficult to obtain both because only 17 codons are unique to the *EcR-B2* mRNA and because all five exons that generate this mRNA are included among the six that generate the *EcR-B1* mRNA (Figures 1B and 2; Talbot et al., 1993). However, comparison of nonleaky B1 and B mutant phenotypes should allow a measure of the EcR-B2 function.

The distribution of *EcR* mutations shown in Figure 2

can be compared to that found for mutations in the human androgen receptor gene, *hAR* (McPhaul et al., 1993). As is the case for *EcR* mutations, virtually all missense mutations are localized to codons for the DBD and LBD. Only one-third of the *EcR-B1* and *hAR* codons encode their DBDs and LBDs (Koelle et al., 1991; McPhaul et al., 1993), yet these two domains account for more than 90% of the missense mutation sites in each gene. Most of the remaining codons encode the N-terminal A/B region adjacent to the DBD and the C-terminal F region adjacent to the LBD (Figure 2), regions that contain virtually no missense mutations in each gene. As might be expected, the paucity of mutations in these regions coincides with the paucity of conserved sequences, yet it is the A/B region that distinguishes the different EcR isoforms. Presumably the functions in this region are not easily susceptible to missense mutations and may be akin to the transcriptional activation function AF-1 found in the A/B region of RARs and RXRs (Nagpal et al., 1993).

Functions of the EcR-B1 Isoform

EcR-B1 mutants are heterochronic in that some tissues initiate metamorphosis normally while others do not. Thus, in *EcR-B1* mutants, leg imaginal discs initiate the process of disc elongation (Figure 4B) while, in contrast, the larval midgut cells as well as the diploid cells of the midgut imaginal islands are blocked in their normal metamorphic responses (Figure 5C). Our finding, that those tissues that are arrested in metamorphic development by *EcR-B1* mutation coincide with those in which EcR-B1 is the predominant isoform in wild type, indicates that EcR-B1 is necessary for their normal metamorphic development. These results support the tissue coordination model (Burtis et al., 1990; Thummel et al., 1990), which proposed that particular combinations of secondary-response effector genes are activated in different target tissues by overlapping combinations of transcription factors encoded by early genes. With the discovery of EcR isoforms and their distribution according to tissue class, the model was amended to specify that the combinations of early-gene transcription factors were determined by tissue-specific combinations of these isoforms (Talbot et al., 1993).

Recently, use of *BR-C* and *E74* mutants combined with detailed molecular analyses of the interactions of the E74A and BR-C Z1 isoforms with the regulatory sequences of the *L71–6* late gene have shown how particular combinations of early-gene transcription factors specify a salivary gland-specific late gene response (Fletcher and Thummel, 1995; Urness and Thummel, 1995; Crossgrove et al., 1996). Our observation, that an *EcR-B1* mutant eliminates the *E74* puff response (which is specific for *E74A* transcription) and modifies the *BR-C* puff response (Figures 6A and 6B), indicates that the EcR-B1 isoform is a necessary component in the chain of command leading to the expression of the *L71–6* late gene. The observation that *EcR-B1* mutation eliminates or severely reduces the puff response of early and early-late genes demonstrates that an EcR isoform is necessary for the ecdysone activation of these genes in vivo.

Functional Differences among the EcR Isoforms

Our use of *EcR-B1* mutant salivary gland nuclei to test for functional differences among the EcR isoforms derived from an earlier test system in which we attempted to rescue *EcR-B1* mutant larvae to adults by the heat-shock expression of each isoform. In this system, a given isoform was produced by heat shock at 12 hr or 24 hr intervals starting with late third instar larvae and continuing until adult flies were formed. While EcR-B1 always rescued best, some rescue by EcR-B2 and EcR-A was also observed at variable lower frequencies that prevented a consistent rank order for second and third place (data not shown). Because a simple plus/minus result was not obtained, and because the relative abundances of the three isoforms could not be usefully assessed during the several days of the test, we moved to the other extreme in designing the test system used here in which single nuclei were examined over a period of a few hours. The fact that some *EcR-B1* mutant larvae were rescued to adulthood by the EcR-A and EcR-B2 isoforms remains, however, and induces the question of its significance as an indicator of a potential overlap in the roles of the different isoforms. Given the abnormally high temporal and tissue abundances incurred during these experiments, we put this result on a par with the finding that the three isoforms can activate with comparable abilities a minimal promoter carrying an ecdysone response element (EcRE) in tissue culture cells (Talbot et al., 1993) or that they exhibit similar EcRE-DNA and hormone-binding coefficients in solution (M. Arbeitman, M. R. Koelle, and D. S. H., unpublished data).

By contrast, the induction of early and early-late genes in *EcR-B1* mutant salivary glands by heat-shock induction of the EcR-B1 isoform was carried out at an EcR-B1 abundance that closely approximates the wild-type level. Indeed, examination of the salivary glands over a longer period following the heat shock frequently resulted in regression of the early and early-late puffs coupled with the activation of late puffs (data not shown), showing that all ranks of the genetic hierarchy induced by the late larval ecdysone pulse can be activated by this heat-shock induction of EcR-B1. When EcR-A was similarly induced, no part of this genetic hierarchy was activated, and EcR-B2 induction produced only an intermediate activation (Figure 6B).

This finding that the EcR isoforms are functionally distinct raises several questions. Perhaps the most obvious is the question of which isoform induces the early genes in tissues where the EcR-A isoform is dominant. For example, the E74A and E75A early-gene isoforms are expressed in imaginal discs (Segraves, 1988; Thummel et al., 1990), yet the predominant ecdysone receptor isoform in discs is EcR-A (Talbot et al., 1993), which fails to significantly activate these early genes in salivary glands (Figure 6B). The question then arises as to whether EcR-A, rather than EcR-B1, which is a minority isoform in discs (Talbot et al., 1993), is used for the ecdysone induction of early genes in these imaginal tissues. This possibility is enhanced by the finding that E74A is present in extracts of *EcR-B1* mutant larvae although it was not detectable in the larval tissues of this mutant (Munroe, 1995).

The possibility therefore exists that tissues with different metamorphic fates are conditioned during their development to employ different EcR isoforms for the induction of the same gene. How could this come about? One possibility is that tissue-specific coactivators may provide the link between the transcription machinery for a given gene and a particular EcR isoform. In this situation, it would be the coactivator that determines which EcR isoform is used to activate the gene. These determinants might be akin to the plethora of putative coactivators recently found for vertebrate nuclear receptors (Mangelsdorf and Evans, 1995). These proteins appear to interact via the C-terminal AF-2 transactivation domain, whereas EcR isoform specificity would have to originate from the N-terminal A/B region. These two conditions could, however, be accommodated by assuming that the specificity of the interaction derived from N-terminal sequences and its stability from the AF-2 interaction.

The advent of mutations that eliminate *EcR-A* and *EcR-B* transcription and detailed analyses of the effects of these and the *EcR-B1* mutation on the ecdysone induction of primary-response genes in specific target tissues should yield a better understanding of the initial determinant for the metamorphic response of these tissues. These mutations, as well as those in the common region, should also be of considerable use in determining the mechanisms underlying these responses, including biochemical and physical chemical studies of the EcR/USP heterodimer and its coactivators and corepressors.

Experimental Procedures

Genetic Screens

To isolate *EcR* alleles, males from an isogenic *cn bw* stock were fed 0.025, 0.037, or 0.05 M EMS in 2% glucose (Lewis and Bacher, 1968). Males were mated to *Bc Elp/CyO* females, and individual *F1 cn bw/CyO* progeny were complementation tested to EcR^{E36Y}/Gla, EcR^{M554fs}/CyO, $EcR^{\Delta E10-12}/CyO$, or *Df(2R)120B/CyO* flies at 25°C. Mutations that completely failed to complement *EcR* for viability were recovered at a rate of 1/1329 for 0.025 M EMS (8 mutations), 1/529 for 0.037 M EMS (18 mutations), and 1/1017 for 0.05 M EMS (1 mutation). *Df(2R)120B* deletes the region from 42A8-10 to 42B1 (R. Kreber and B. S. G., unpublished data).

Denaturing Gradient Gel Electrophoresis and Sequence Analysis

Genomic DNA from *EcR* protein-coding sequences was amplified by PCR from flies heterozygous for *EcR* mutations and one of two balancer chromosomes (*SM6b* or *In(2LR)Gla*) using PCR primers 20 nucleotides (nt) in length. One member of each PCR primer pair included a 40 nt GC clamp (Sheffield et al., 1989). PCR products were electrophoresed on 6.5% acrylamide gels across an increasing gradient of denaturant at 60°C (Myers et al., 1987). Gels were stained with ethidium bromide to detect DNA species with altered mobility relative to PCR products amplified from parental chromosomes. PCR products were cloned and sequenced by the dideoxy chain termination method. A minimum of six independent clones was sequenced for each mutant. EcR^{M554fs} is a 22 nt deletion starting at nt 2729 (Koelle et al., 1991). EcR^{W69R} is a 37 nt deletion starting at nt 2743. $EcR^{\Delta S347-A497}$ is a 167 nt deletion that entirely removes exon 5, starting 2 nt upstream of the intron/exon boundary and extending to 12 nt downstream of the exon/intron boundary.

Lethal Phase Determination

EcR mutants were marked with yellow (*y*) using a *CyO,y+* chromosome. Eggs were collected on agar plates for a 6 hr period 2–4 days following the mating of 25 *yw; EcR/CyO,y+* males to 25 *yw;* EcR^{M554fs}*/CyO,y+* virgin females at 25°C. The sample size for each analysis was 200 eggs, representing a Mendelian expectation of 50 *EcR* mutant animals. At 36 hr after egg laying (AEL), the numbers of hatched eggs and living *EcR* mutant (*y*) first instar larvae were scored, and living *y* larvae were placed in yeast paste on a fresh agar plate at 25°C. Animals were scored for viability and placed on fresh plates at mid-second instar (60 hr AEL) and mid-third instar (96 hr AEL), and later were scored for pupariation and adult eclosion. Two mutants (EcR^{C30Y} and EcR^{E27Q}) were inviable or infertile over *CyO,y+* and were not tested. To generate EcR^{M554fs}*/Df(2R)nap11* hemizygotes (Figure 3) and EcR^{M554fs} homozygotes, EcR^{M554fs}*/Oregon R* males were crossed to either *Df(2R)nap11/Oregon R* or EcR^{M554fs}*/Oregon R* females.

Examination of Internal Tissues and Polytene Chromosome Cytology

For examination of internal tissues, late-stage *EcR-B1* mutants were selected for dissection after the gap at the posterior end of the animal (see Figure 3D) had reached its maximal extent. This event is achieved by 6 hr after the larvae cease movement. Cessation of movement of the *EcR-B1* mutant larvae is roughly comparable to the white prepupa stage in wild-type animals. Larvae were dissected in PBS and fixed in 2% paraformaldehyde for 30 min. Tissues were stained briefly with DAPI (1 μg/ml), washed with PBS, and mounted for microscopy.

For polytene chromosome cytology, larvae produced from a cross of *yw;* EcR^{M554fs}*/CyO,y+* males to *yw;* EcR^{M554fs}*/CyO,y+* females were grown at 18°C in medium containing 0.05% bromphenol blue. *EcR* mutant larvae (*yw;* EcR^{M554fs}*/*EcR^{M554fs}) were distinguished from siblings by the *y* marker and staged by clearing of the larval gut (Andres and Thummel, 1994). The blue-gut stage corresponds to the onset of wandering before the ecdysone titer rises sharply and the early puffs are induced. Larvae at the clear-gut stage have initiated the ecdysone-induced puffing of early-puff genes (Andres and Thummel, 1994). Salivary glands were dissected in PBS, fixed in 45% acetic acid for 1.5–2 min, and stained in a drop of lacto-acetic orcein for 4–5 min. Squashes were examined using a Zeiss Axiophot microscope. Puffing activity was measured as the ratio of the maximum width of the puff to that of a previously characterized reference band (Ashburner, 1974; Belyaeva et al., 1981). Each column of Figures 6A and 6B represents the mean puff size from four separate nuclei from each of five animals, for a total of 20 measurements. The error bar shows the standard error.

EcR Isoform Rescue of Puffing in an *EcR-B1* Mutant

EcR-B1 mutant larvae (*yw;* EcR^{M554fs}*/*EcR^{M554fs}*; hs EcR-x/+*, where *x* is A, B1, or B2) were separated into three groups according to amount of blue in the larval gut. The middle group was selected to ensure the best probability of choosing larvae with a high ecdysone titer (Andres and Thummel, 1994). Larvae were subjected to a 45 min heat shock at 37°C followed by a 4 hr recovery period at 22°C. Puffing activity was measured as described above.

Quantitation of EcR Protein Following Heat-Shock Induction

Levels of EcR protein present in salivary gland nuclei were examined for all three heat-shock isoform lines: *yw;* EcR^{M554fs}*/CyO,y+*; *hs-EcR-*$B1^{1}$*/hs-EcR-*A^{PE+}*, yw; EcR*^{M554fs}*/CyO,y+*; *hs-EcR-B1/hs-EcR-B1*, and *yw;* EcR^{M554fs}*/CyO,y+*; *hs-EcR-*$B2^{E1}$*/hs-EcR-*$B2^{E1}$. Larvae were examined either without heat shock or after a 45 min heat shock followed by a 3 hr recovery period. Larvae were dissected in PBS, fixed in 2% paraformaldehyde for 30 min and stained as described (Koelle et al. 1991). The EcR common region primary antibody DDA2.7 was diluted 1:5, and the fluorescein-conjugated secondary antibody was diluted 1:200. Salivary glands were dissected in PBS and mounted on glass slides using spacers between slide and cover slip to avoid crushing salfvary gland cells. Attenuation and voltage of the Molecular Dynamics confocal microscope used to quantitate EcR protein levels were held constant. Staining intensities were quantitated for four nuclei from each experimental group by selecting a central 0.7 micron cross section from a stack of 8 sections. Western blots of proteins extracted from each experimental group following heat shock were probed with the DDA2.7 common-region

antibody, and proteins with molecular weights corresponding to the proper isoform were detected.

Acknowledgments

We thank Brandon Hipsher, Ken Relloma, and Robert Kreber for expert technical assistance and Michael Koelle, Scot Munroe, Ed Stephenson, and J. Willis for helpful comments on the manuscript. This work was supported by NSF and NIH grants to D. S. H., NIH grant #GM43100 to B. G., NIH grant #GM53681 to M. B., a Helen Hay Whitney Fellowship and an NIH Fellowship for training in Tumor Biology to M. B., and an NSF Graduate Fellowship to W. S. T.

Received August 29, 1997; revised November 10, 1997.

References

Andres, A.J., and Thummel, C.S. (1994). Methods for quantitative analysis of transcription in larvae and prepupae. In Drosophila melanogaster: Practical Uses in Cell and Molecular Biology, L.S.B. Goldstein and E.A. Fyrberg, eds. (San Diego, CA: Academic Press), pp. 565–573.

Andres, A.J., and Thummel, C.S. (1995). The Drosophila 63F early puff contains *E63-1*, an ecdysone-inducible gene that encodes a novel Ca^{2+}-binding protein. Development *121*, 2667–2679.

Andres, A.J., Fletcher, J.C., Karim, F.D., and Thummel, C.S. (1993). Molecular analysis of the initiation of insect metamorphosis: a comparative study of Drosophila ecdysteroid-regulated transcription. Dev. Biol. *160*, 388–404.

Ashburner, M. (1974). Sequential gene activation by ecdysone in polytene chromosomes of Drosophila melanogaster. II. The effects of inhibitors of protein synthesis. Dev. Biol. *39*, 141–157.

Beato, M., Herrlich, P., and Schutz, G. (1995). Steroid hormone receptors: many actors in search of a plot. Cell *83*, 851–857.

Belyaeva, E.S., Vlassova, I.E., Biyasheva, Z.M., Kakpakov, V.T., Richards, G., and Zhimulev, I.F. (1981). Cytogenetic analysis of the 2B3–4 to 2B11 region of the X-chromosome of Drosophila melanogaster. II. Changes in 20-OH ecdysone puffing caused by genetic defects of puff 2B5. Chromosoma *84*, 207–219.

Burtis, K.C., Thummel, C.S., Jones, C.W., Karim, F.D., and Hogness, D.S. (1990). The Drosophila 74EF early puff contains E74, a complex ecdysone-inducible gene that encodes two ets-related proteins. Cell *61*, 85–99.

Crossgrove, K., Bayer, C.A., Fristrom, J.W., and Guild, G.M. (1996). The Drosophila Broad-Complex early gene directly regulates late gene transcription during the ecdysone-induced puffing cascade. Dev. Biol. *180*, 745–758.

Dai, J.D., and Gilbert, L.I. (1991). Metamorphosis of the corpus allatum and degeneration of the prothoracic glands during the larval-pupal-adult transformation of Drosophila melanogaster: a cytophysiological analysis of the ring gland. Dev. Biol. *144*, 309–326.

Dibello, P.R., Withers, D.A., Bayer, C.A., Fristrom, J.W., and Guild, G.M. (1991). The Drosophila Broad-Complex encodes a family of related proteins containing zinc fingers. Genetics *129*, 385–397.

Fletcher, J.C., and Thummel, C.S. (1995). The Drosophila *E74* gene is required for the proper stage- and tissue-specific transcription of ecdysone-regulated genes at the onset of metamorphosis. Development *121*, 1411–1421.

Fristrom, D., and Fristrom, J.W. (1993). The metamorphic development of the adult epidermis. In The Development of Drosophila melanogaster, M. Bate and A. Martinez-Arias, eds. (Cold Spring Harbor, NY: Cold Spring Harbor Laboratory Press), pp. 843–898.

Giguere, V. (1994). Retinoic acid receptors and cellular retinoid binding proteins: complex interplay in retinoid signaling. Endocr. Rev. *15*, 61–79.

Jiang, C., Baehrecke, E.H., and Thummel, C.S. (1997). Steroid regulated programmed cell death during Drosophila metamorphosis. Development, in press.

Kastner, P., Mark, M., and Chambon, P. (1995). Nonsteroid nuclear receptors: what are genetic studies telling us about their role in real life? Cell *83*, 859–869.

Koelle, M.R. (1992). Molecular analysis of the *Drosophila* ecdysone receptor complex. PhD thesis, Stanford University, Stanford, CA.

Koelle, M.R., Talbot, W.S., Segraves, W.A., Bender, M.T., Cherbas, P., and Hogness, D.S. (1991). The Drosophila *EcR* gene encodes an ecdysone receptor, a new member of the steroid receptor superfamily. Cell *67*, 59–77.

Lewis, E.B., and Bacher, F. (1968). Method of feeding ethyl methane sulfonate (EMS) to Drosophila males. Dros. Inf. Ser. *43*, 193.

Madhavan, M.M., and Madhavan, K. (1980). Morphogenesis of the epidermis of adult abdomen of Drosophila. J. Embryol. Exp. Morph. *60*, 1–31.

Mangelsdorf, D.J., and Evans, R.M. (1995). The *RXR* heterodimers and orphan receptors. Cell *83*, 841–850.

Mangelsdorf, D.J., Thummel, C., Beato, M., Herrlich, P., Schutz, G., Umesono, K., Blumberg, B., Kastner, P., Mark, M., Chambon, P., and Evans, R. (1995). The nuclear receptor superfamily: the second decade. Cell *83*, 835–839.

McPhaul, M.J., Marcelli, M., Zoppi, S., Griffin, J.E., and Wilson, J.D. (1993). Genetic basis of endocrine disease 4: the spectrum of mutations in the androgen receptor that causes androgen resistance. J. Clin. Endocrinol. Metab. *76*, 17–23.

Munroe, S.D. (1995). Roles of the E74 proteins in the ecdysone response of Drosophila. PhD thesis, Stanford University, Stanford, CA.

Myers, R.M., Maniatis, T., and Lerman, L.S. (1987). Detection and localization of single base changes by denaturing gradient gel electrophoresis. Meth. Enzymol. *155*, 501–527.

Nagpal, S., Friant, S., Nakshatri, H., and Chambon, P. (1993). RARs and RXRs: evidence for two autonomous transactivation functions (AF-1 and AF-2) and heterodimerization in vivo. EMBO J. *12*, 2349–2360.

Refetoff, S., Weiss, R.E., Usala, S.J., and Hayashi, Y. (1994). The syndromes of resistance to thyroid hormone: update 1994. Endocrin. Rev. *15*, 336–343.

Riddiford, L.M. (1993). Hormones and Drosophila development. In The Development of Drosophila melanogaster, M. Bate and A. Martinez-Arias, eds. (Cold Spring Harbor, NY: Cold Spring Harbor Laboratory Press), pp. 899–940.

Robinow, S., Talbot, W.S., Hogness, D.S., and Truman, J.W. (1993). Programmed cell death in the Drosophila CNS is ecdysone-regulated and coupled with a specific ecdysone receptor isoform. Development *119*, 1251–1259.

Russell, S., and Ashburner, M. (1996). Ecdysone-regulated chromosome puffing in Drosophila melanogaster. In Metamorphosis: Postembryonic Reprogramming of Gene Expression in Amphibian and Insect Cells, L.I. Gilbert, J.R. Tata, and G.B. Atkinson, eds. (New York: Academic Press), pp. 109–144.

Segraves, W.A. (1988). Molecular and genetic analysis of the E75 ecdysone-responsive gene of Drosophila melanogaster. PhD thesis, Stanford University, Stanford, CA.

Segraves, W., and Hogness, D.S. (1990). The *E75* ecdysone-inducible gene responsible for the 75B early puff in Drosophila encodes two new members of the steroid receptor superfamily. Genes Dev. *4*, 204–219.

Sheffield, V.C., Cox, D.R., Lerman, L.S., and Myers, R.M. (1989). Attachment of a 40-base-pair G + C-rich sequence (GC-clamp) to genomic DNA fragments by the polymerase chain reaction results in improved detection of single-base changes. Proc. Natl. Acad. Sci. USA *86*, 232–236.

Skaer, H. (1993). The alimentary canal. In The Development of Drosophila melanogaster, M. Bate and A. Martinez-Arias, eds. (Cold Spring Harbor, NY: Cold Spring Harbor Laboratory Press), pp. 941–1012.

Talbot, W.S., Swyryd, E.A., and Hogness, D.S. (1993). Drosophila tissues with different metamorphic responses to ecdysone express different ecdysone receptor isoforms. Cell *73*, 1323–1337.

Thummel, C.S. (1995). From embryogenesis to metamorphosis: the regulation and function of Drosophila nuclear receptor superfamily members. Cell *83*, 871–877.

Thummel, C.S., Burtis, K.C., and Hogness, D.S. (1990). Spatial and temporal patterns of *E74* transcription during Drosophila development. Cell *61*, 101–111.

Urness, L.D., and Thummel, C.S. (1995). Molecular analysis of a steroid-induced regulatory hierarchy: the Drosophila E74A protein directly regulates L71–6 transcription. EMBO J. *14*, 6239–6246.

Yao, T.P., Segraves, W.A., Oro, A.E., McKeown, M., and Evans, R.M. (1992). Drosophila ultraspiracle modulates ecdysone receptor function via heterodimer formation. Cell *71*, 63–72.